Catal Lett (2008) 122:115–120
DOI 10.1007/s10562-007-9355-7

Study on Copper-based Catalysts for Synthesis of *N*,*N*′-bis (1,4-dimethylpentyl)-*p*-phenylenediamine from Reductive Alkylation of *p*-Nitroaniline with 5-Methyl-2-hexanone

Zhen Dong Pan · Yun Jie Ding · Li Yan · Xian Ming Li · Gui Ping Jiao · Hong Yuan Luo

Received: 19 September 2007 / Accepted: 13 November 2007 / Published online: 12 December 2007

Abstract The reductive alkylation of *p*-nitroaniline with 5-methyl-2-hexanone over copper-based catalysts was investigated. Furthermore, the catalysts were characterized using the techniques of XRD, H_2–N_2O titration, H_2-TPR, NH_3-TPD and pyridine-FTIR. The results showed that the addition of Mn, Ba and La into Cu–SiO_2 catalyst played an important role in the improvement of the selectivity towards *N*,*N*′-bis(1,4-dimethylpentyl)-*p*-phenylenediamine (BMPPD). The highest selectivity towards BMPPD over 58CuO–9MnO_2–BaO–1La_2O_3–30SiO_2 (wt.%) catalyst could be ascribed to the best dispersion of copper (i.e., the highest hydrogenation ability) and the most amounts of the surface Lewis acidic sites.

Keywords Copper-based catalysts · *N*,*N*′-bis(1,4-dimethylpentyl)-*p*-phenylenediamine · *p*-Nitroaniline · 5-Methyl-2-hexanone · Dispersion · Lewis acidic sites

1 Introduction

N,*N*′-disubstituted *p*-phenylenediamines are the most widely used and the most effective antiozonant and antioxidant stabilizers for the protection of rubber, plastics, gasoline and lubricants [1–4]. For example, *N*,*N*′-bis(1,4-dimethylpentyl)-*p*-phenylenediamine (BMPPD) can capitally suppress degradation of ozone attack on rubber compounds in static. *N*,*N*′-disubstituted *p*-phenylenediamines can be efficiently produced by one step synthesis from the reductive alkylation of *p*-nitroaniline with ketones in the presence of hydrogen and a transition metal based catalyst or noble metal based catalyst [5]. However, some problems such as environmental pollution of poisonous copper–chromite catalysts [6, 7] and high costs of noble metal based catalysts [8–11] are still open. Therefore, the study and development of efficient, economical and environment-friendly catalyst are necessary.

In this paper, the effect of the environmental-friendly Mn, Ba and La on copper-based catalysts was investigated by techniques of XRD, H_2–N_2O titration, H_2-TPR, NH_3-TPD and pyridine-FTIR, and their catalytic properties were evaluated in reductive alkylation of *p*-nitroaniline with 5-methyl-2-hexanone in the presence of hydrogen. The study found that the addition of Mn, Ba and La played an important role in the selective synthesis of BMPPD from reductive alkylation of *p*-nitroaniline with 5-methyl-2-hexanone. The characterization results turned out that the copper dispersion and the acidic properties of copper-based catalysts were enhanced by the addition of Mn, Ba and La and so the selectivity towards BMPPD was improved.

2 Experimental

2.1 Catalyst Preparation

A 70 mL aqueous solution of NaOH (3 M) was added to a 200 mL aqueous solution containing 17.6 g $Cu(NO_3)_2 \cdot 3H_2O$, 3.7 g $Mn(NO_3)_2$ (50 wt.%, aqueous solution), 0.34 g $Ba(NO_3)_2$ and 0.23 g $La(NO_3)_3 \cdot nH_2O$ (44 wt.% La_2O_3)

Z. D. Pan · Y. J. Ding (✉) · L. Yan · X. M. Li · G. P. Jiao · H. Y. Luo
Dalian Institute of Chemical Physics, Chinese Academy of Sciences, Dalian 116023, P.R. China
e-mail: dyj@dicp.ac.cn

Z. D. Pan · X. M. Li · G. P. Jiao
Graduate School of Chinese Academy of Sciences, Beijing 100039, P.R. China

to form co-precipitates. The co-precipitates were allowed to age for 4 h at 343 K, following addition of 11.3 g of aqueous silica sol (26.6 wt.% SiO_2, China medicine (group) shanghai chemical reagent Co.) to the solution. The resulting precipitate was recovered by filtration, followed by washing with de-ionized water and drying for 12 h at 393 K. Then, the dry powder was pressed and sieved to 20–40 mesh particles. The particles were calcined in a muffle furnace in a static air atmosphere by increasing the temperature from ambient temperature to 773 K at a rate of 10 K min^{-1} and kept at 773 K for 6 h to produce 58CuO–9MnO_2–BaO–1La_2O_3–30SiO_2 (wt.%), denoted as catalyst A. 6CuO–9MnO_2–31SiO_2 and 65CuO–35SiO_2 (wt.%) denoted as catalysts B and C, respectively, were prepared by using the same method as preparing catalyst A with corresponding nitrates.

2.2 Catalytic Test

Reductive alkylation of *p*-nitroaniline with 5-methyl-2-hexanone were carried out in a fixed-bed micro-reactor under 383 K, 5.0 MPa, LHSV = 1.0 h^{-1}, GHSV = 600 h^{-1} (pure H_2) and the ratio of *p*-nitroaniline to 5-methyl-2-hexanone = 1:12 (molar ratio) which was pumped with a double-plunger micro-pump. Before reaction, all the catalysts were in-situ activated at 548 K for 3 h in a flow of pure H_2. The outlet products first cooled down to 273 K in a cold trap and were analyzed by off-line HP-6890 gas chromatography equipped with FID and a 30 m SE-54 capillary column.

2.3 Catalyst Characterization

Powder X-ray diffraction (XRD) analysis was performed on PANalytical X'Pert PRO XRD using CuKα radiation filtered by a graphic monochromator at a setting of 40 kV and 40 mA in the scanning angle (2θ) range of 10–100° at scanning speed of 14° min^{-1}. The sample was reduced by pure H_2 for 3 h at 548 K to obtain XRD patterns of reduced catalysts.

H_2–N_2O titration experiments were performed on a Quantachrome Autosorb-1 apparatus. The sample was first reduced by a 10% H_2–Ar gas mixture at 573 K for 1 h. Surface oxidation was performed by dissociative adsorption of nitrous oxide (10% N_2O/N_2) onto the reduced catalyst at 393 K for 20 min. Complete oxidation of the reduced catalyst was carried out with a mixture of 20% O_2/N_2 at 723 K for 60 min. The hydrogen consumption after surface oxidation, *X*, and after complete bulk oxidation of the same catalyst sample, *Y*, were obtained from reducing the sample by a 10% H_2–Ar gas mixture and monitoring simultaneously the signal of H_2 (m/z = 2) with a mass spectrometer detector (Prisma).

H_2 temperature programmed reduction (H_2-TPR) measurements were performed on a Micromeritics Autochem 2910 apparatus. One hundred milligrams of catalyst was placed in a quartz reactor and reduced by a 10% H_2–Ar gas mixture in a flow rate of 50 mL/min with temperature ramping at 10 K/min. After exiting the reactor, the effluent was led via a cooling trap immerged in a mixture solution of liquid nitrogen and *i*-pentanol to remove H_2O, and the hydrogen consumption was subsequently recorded with a thermal conductivity detector and calibrated using TPR of copper oxide (CuO) at the same conditions.

Temperature programmed desorption of adsorbed ammonia (NH_3-TPD) was performed in a Micromeritics Autochem 2910. The sample (0.3 g) was reduced in pure H_2 for 1 h at 573 K. After cooling to 373 K under continuous flow of helium, the sample was adsorbed with NH_3 using pulse model until saturation. Then the temperature was linearly increased from 373 to 873 K at 10 K/min, following the signal of NH_3 (m/z = 16) with a mass spectrometer detector (Balzers OmniStar 300).

Fourier transform infrared spectra of adsorbed pyridine (pyridine-FTIR) were performed on a BRUKER EQUINOX 55 Spectrometer equipped with a DTGS detector. The sample was first vacuated for 1 h at 723 K and then cooled to room temperature. An FT–IR spectrum (denoted as spectrum A) of the catalyst was recorded. Subsequently, after adsorption of pyridine for 20 min at room temperature, the sample was vacuated for 0.5 h at 423 K or 623 K (10^{-2} Pa), and then spectrum B was recorded. All spectra were recorded at 4 cm^{-1} resolution with 16 co-added scans. Subtracting spectrum A from spectrum B gave a final spectrum.

3 Results and Discussion

3.1 Reaction Results

The conversions of *p*-nitroaniline over all catalysts were nearly 100%, which were not given in Table 1. The selectivity towards BMPPD on catalyst C without any additives was 92.1%. There were more *p*-phenylenediamine (PD), *N*-(1,4-dimethylpentyl)-*p*-phenylenediamine (DMPPD) and other by-products. The selectivity towards BMPPD on catalyst B containing the additive Mn was 95.7% and that towards DMPPD decreased. Meanwhile, *N*,*N*,*N*′-tri-(1,4-dimethylpentyl)-*p*-phenylenediamine (TMPPD) appeared. As seen from Table 1, after the addition of Ba and La into catalyst B, DMPPD over catalyst A disappeared. Moreover, other by-products distinctly decreased. However, the selectivity towards BMPPD further increased and reached 97.4%, except that TMPPD was slightly higher.

Table 1 Product distribution on catalysts A, B and C

Catalysts	Selectivity of products, %				
	PD	DMPPD	BMPPD	TMPPD	OB
A	0	0	97.4	1.4	1.2
B	0	0.5	95.7	0.5	3.3
C	1.7	1.2	92.1	0	5.0

PD: *p*-phenylenediamine, DMPPD: *N*-1,4-dimethylpentyl-*p*-phenylenediamine, BMPPD: *N*,*N*′-bis(1,4-dimethylpentyl)-*p*-phenylenediamine, TMPPD: *N*,*N*,*N*′-tri-(1,4-dimethylpentyl)-*p*- phenylenediamine and OB: other byproducts

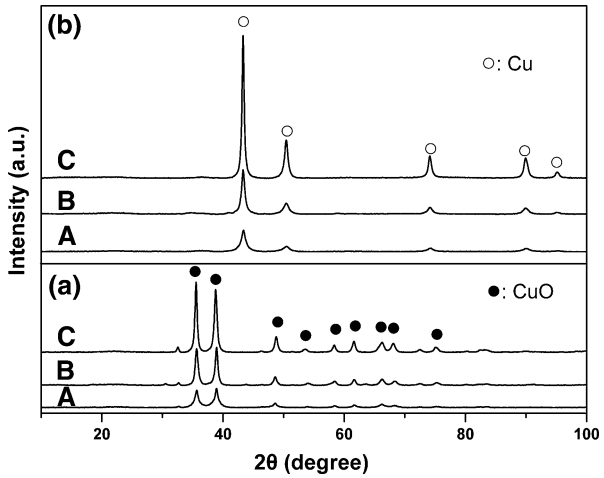

Fig. 1 XRD patterns of unreduced (**a**) and reduced (**b**) catalysts A, B and C

3.2 Characterization of Catalysts

3.2.1 XRD Study

Figure 1 gives the XRD patterns of unreduced (a) and reduced (b) catalysts A, B and C. There was not a broad peak at $2\theta = 22.5°$ attributed to amorphous silica over all catalysts previously reported [12, 13], which was possibly due to amorphous silica being completely highly dispersed. It was obvious that diffraction peaks of other metal oxides except for CuO were not observed in all unreduced catalysts, implying that other metal oxides of catalysts A and B were highly dispersed. The intensities of CuO diffraction peaks decreased drastically in the following sequence: C > B > A, which indicated that the Mn, Ba and La could improve distinctly the CuO dispersion. Moreover, it was obvious that only Cu diffraction peaks were observed over all reduced catalysts and their intensities were in the same sequence as that of CuO. These results suggest that there are strong additive effects of Mn, Ba and La on Cu dispersion of Cu–SiO_2 catalyst, which might result in the better selectivity towards BMPPD in reductive alkylation of *p*-nitroaniline with 5-methyl-2-hexanone.

3.2.2 H_2–N_2O Titration

In order to determine the copper surface exposed and the dispersion in the reduced samples, H_2–N_2O titration method was used. Dispersion (D) and copper surface area (S) and average volume-surface diameter of copper particles ($d_{v.s.}$) were calculated from hydrogen consumption (X, Y) according to the method described by Guerreiro et al. [14], i.e., $D = 2 \cdot X/Y$, $S \cong 1353\ X/Y$ (m^2/g Cu), $d_{v.s.} \cong 0.5 \cdot Y/X$ (nm). D, S and $d_{v.s.}$ of various catalysts are summarized in Table 2. It was clearly noted that the dispersion and copper surface area decreased in the following sequence: A > B > C and average volume-surface diameter of copper particles was in the contrary sequence. This indicates that the copper dispersion was enhanced by the addition of Mn, Ba and La into catalyst C. The densities (ρ) of the surface Cu in the catalysts which were calculated from D and BET surface area are also presented in Table 2. Because BET surface area decreased drastically in the following sequence: A > B > C, so ρ was in the contrary sequence. Usually, high BET surface area favored the catalytic reactions, therefore, catalyst A had high selectivity towards BMPPD, although it had low ρ.

3.2.3 H_2-TPR Analysis

H_2-TPR profiles of catalysts A, B and C are presented in Fig. 2. The catalysts exhibited two reduction peaks at

Table 2 Textural and chemical properties of catalysts A, B and C

Catalysts	D (%)	S (m^2/g Cu)	$d_{v.s.}$ (nm)	ρ[a] (10^{-2} mmol/m^2)	Quantity of H_2 consumption[b] (mmol g^{-1})	
					Peak I	Peak II
A	21.9	148	4.56	1.17	3.0	4.2
B	18.5	125	5.41	2.06	1.8	5.8
C	15.4	104	6.48	2.32	1.4	6.6

[a] Calculated from D and BET surface area

[b] Measured by H_2-TPR

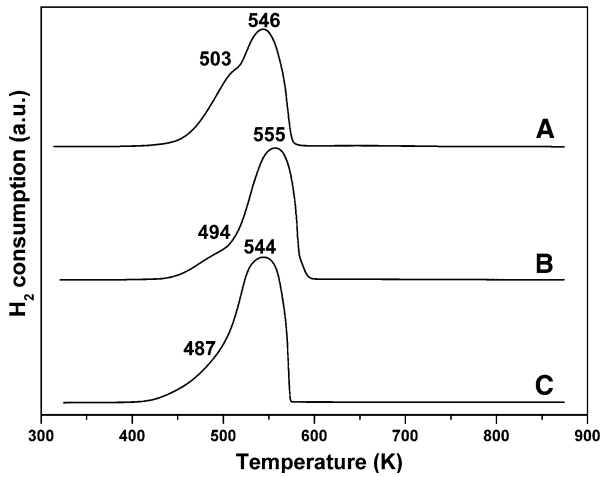

Fig. 2 H_2-TPR profiles of catalysts A, B and C

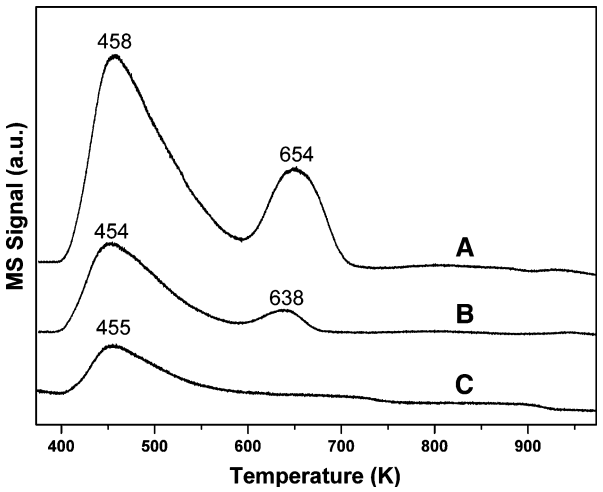

Fig. 3 NH_3-TPD spectra of catalysts A, B and C

temperature region of 420–510 K (referred to as peak I) and 540–600 K (peak II). Obviously, the peak area of peak II was much bigger than that of peak I. Bond et al. ever reported [15] the stepwise reduction of Cu^{2+} on $CuCl_2/SiO_2$, namely, $Cu^{2+} \rightarrow Cu^{1+} \rightarrow Cu^0$, the ratio of the peak areas being close to 1:1. Our results are not coincident with their result. This means that there probably were two different CuO species. It had been reported that more than one form of copper species existed on the surface of catalysts and various species would play different roles in catalytic reactions [12, 16]. Similarly, the peak I would be attributed to the reduction of highly dispersed CuO species and the peak II should be ascribed to the reduction of CuO clusters. In order to well understand the effects of Mn, Ba and La on the catalytic properties of catalysts B and A, the H_2 consumption quantities of each peak per gram catalyst were calculated from the TPR profiles and listed in Table 2. The H_2 consumption quantities of peak I over catalyst B was slightly higher than that of catalyst C. However, the H_2 consumption quantities of the peak I over catalyst A was much higher than that of catalyst B, which obviously illuminated that catalyst A contained much more highly dispersed CuO species than catalysts C and B, which was consistent with XRD and H_2–N_2O titration results. Therefore, it was substantiated that the addition of Mn, Ba and La into catalyst C played an important role in increasing the dispersion Cu species and the number of metallic sites.

3.2.4 NH_3-TPD Results

NH_3-TPD is usually used to measure the acidic properties of the catalyst. The strength of the acidity is characterized by the temperature of desorption peak. On the other hand, the number of acidic sites is measured by desorption peak intensity and area [17]. NH_3-TPD spectra of in situ reduced catalysts A, B and C are shown in Fig. 3. A desorption peak representing weak acidic sites was recorded at ca. 458, 454 and 455 K on the surface of the catalysts A, B and C, respectively. However, there was a desorption peak representing strong acidic sites at ca. 654 K and 638 K on the surface of catalysts A and B, respectively, almost no peak was observed in the same temperature range on catalyst C, which implied that strong acidic sites only presented on catalysts A and B and their strength of the acidity on the surface of catalyst A was slightly stronger than that of catalyst B. It was worthy noting that two NH_3 desorption peak intensity or area assignable to weak acidic sites and strong acidic sites were in the following sequence: A > B > C. This result indicates that the number of surface strong acidic and weak acidic sites increased with the addition of Mn, Ba and La into catalyst C.

3.2.5 FT-IR Spectroscopy

The infrared spectra of pyridine adsorbed on the samples in the spectral region of 1,700–1,300 cm^{-1} give information that the wave number of the bands at 1,464–1,447 cm^{-1}, which is sensitive to the acidity strength of the Lewis acid sites, and the intensity of the bands at 1,634–1,600 cm^{-1}, which characterizes the number of such sites, and the bands at 1,550–1,535 cm^{-1} and ca. 1,640 cm^{-1} characterize Brönsted acid sites [18].

Figure 4 presents pyridine-FTIR of A, B and C catalysts evacuated at 423 K and 623 K after pyridine adsorption respectively. Two bands at 1,448–1,450 cm^{-1} and ca. 1,610 cm^{-1} corresponding to Lewis acidic sites were observed after evacuation at 423 K. After evacuation

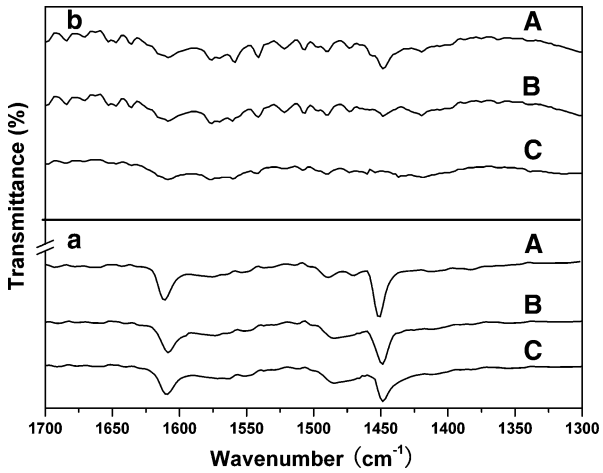

Fig. 4 Pyridine-FTIR spectra of catalysts A, B and C (evacuated at (**a**): 423 K; (**b**): 623 K)

at 623 K, catalyst A had weak bands, catalyst B had weaker bands than catalyst A and catalyst C had no bands. The wave number of the band at ca. 1,448 cm^{-1} over catalysts B and C was almost identical, implying that there was little difference in the strength of the surface Lewis acidity. However, the wave number of the band at ca. 1,450 cm^{-1} over catalyst A was slightly shift to higher wave number than that of catalyst B, which implied that the strength of surface Lewis acid sites of catalyst A was stronger than that of catalysts B and C. The intensity of the band at ca. 1,610 cm^{-1} was in the following sequence: A > B > C, which indicated that the number of surface Lewis acidity sites decreased in the same sequence. These results are consistent with the results of NH_3-TPD. It was obviously that there were no bands at 1,550–1,535 cm^{-1} and ca. 1,640 cm^{-1} observed in pyridine-FTIR spectra, thus no detectable Brönsted acid sites could be identified.

We had reported that the reaction pathway of the reductive alkylation of *p*-nitroaniline with 2-butanone [5]. Similarly, the reaction pathway of the reductive alkylation of *p*-nitroaniline with 5-methyl-2-hexanone could be proposed in Scheme 1. Four steps are involved in the reductive alkylation as follows: (I) hydrogenation of *p*-nitroaniline to PD on the metallic sites; (II) nucleophilic addition of PD with 5-methyl-2-hexanone to form *N*,*N*′-di-(1,4-dimethyl-1-hydroxypentyl)-*p*-phenylene diamine on the surface Lewis acid sites; (III) dehydration of *N*,*N*′-di-(1,4-dimethyl-1-hydroxypentyl)-*p*-phenylenediamine to *N*,*N*′-di-(1,4-dimethyl pentylidene)-*p*-phenylenediamine on the surface Lewis acid sites; (IV) hydrogenation of *N*,*N*′-di-(1,4-dimethylpentylidene)-*p*-phenylenediamine to BMPPD on the metallic sites. As well known, the hydrogenation of nitro group (step I) and imine (step IV) was usually accomplished on the metallic sites [19]. The courses of nucleophilic addition (step II) and the elimination of water (step III), namely, the condensation of primary amine with ketone, could achieved on Lewis acid sites [5]. In order to acquire the highly efficient synthesis of BMPPD from reductive alkylation of *p*-nitroaniline with 5-methyl-2-hexanone, the amount of the surface Lewis acidic sites as well as the dispersion of Cu in the copper-based catalysts should be matched among the reaction steps above mentioned. For example, too large number of Lewis acid sites could lead to too high rate of condensation, in turn, resulted in high selectivity towards tri-alkyl, tetra-alkyl *p*-phenylenediamine and imine. In contrast, too small number of the Lewis acid sites could lead too low rate of condensation, accordingly, high selectivity towards mono-alkylated *p*-phenylenediamine and PD. In addition, the difference of Cu dispersion induced different hydrogenation capability. For example, a little number of metallic sites could lead to low rate of hydrogenation, consequently, high selectivity towards mono-alkylated *p*-phenylenediamine and imine was obtained.

Scheme 1 Reaction pathway of the reductive alkylation of *p*-nitroaniline with 5-methyl-2-hexanone

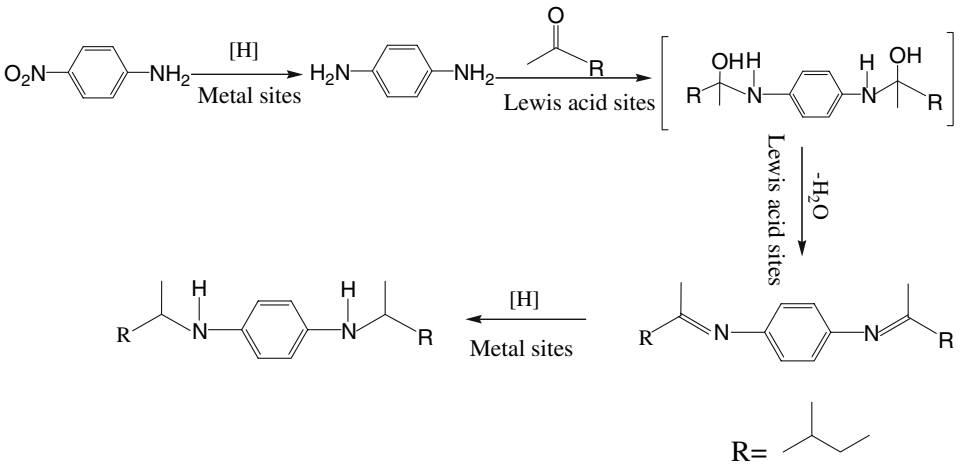

The catalyst C had the least amount of the surface Lewis acidic sites among the catalysts, being unfavorable of the condensation, so there showed the lowest selectivity to BMPPD in the products. Furthermore, the catalyst C showed the lowest dispersion of Cu and the lowest hydrogenation ability among the catalysts and was not in favor of the hydrogenation, so the most by-products like imine were formed. Therefore, catalyst C exhibited the highest selectivity towards DMPPD and the lowest selectivity towards BMPPD. The catalyst B with more surface Lewis acid sites and better dispersion of Cu exhibited higher selectivity towards BMPPD than catalyst C. The catalyst A possessed the most amount of the surface Lewis acidic sites and the best dispersion of Cu (i.e., the highest hydrogenation ability), consequently, resulted in the highest selectivity towards BMPPD among the catalysts.

4 Conclusions

Catalyst A containing Mn, Ba and La possessed the best dispersion of copper (i.e., the highest hydrogenation ability) and the most amounts of the surface Lewis acidic sites, so it exhibited the highest selectivity to BMPPD from the reductive alkylation of *p*-nitroaniline with 5-methyl-2-hexanone.

References

1. Choi SS (1997) J Appl Polym Sci 65:117
2. Reynolds MP, Greenfield H (1996) Chem Ind 68:343
3. Cataldo F (2002) Eur Polym J 38:885
4. Gupta AA, Puri SK, Chand S, Sharma VK, Manoharan R, Prashad R, Raje NR, Bratnagar AK (2005) US patent 2,005,091,914
5. Pan ZD, Ding YJ, Jiang DH, Li XM, Jiao GP, Luo HY (2007) Appl Catal A Gen 330:43
6. Ward S, Lamb SA, Hodgson MAE (1954) GB patent 712,100
7. Jaros A, Dolezel P, Orlik I, Halomi M, Dudek I, Pasek J, Gabarik M (1988) Czech CS 257,400
8. Hanai M, Tada K, Kodear N, Takada T (1982) JP patent 57,156,446
9. Banerjee AA, Mukesh D (1988) J Chem Soc Chem Commun 18:1275
10. Kodear N, Tada K, Hirabayashi K, Yamamoto K, Takada T (1983) JP patent 58,194,843
11. Symon T (1980) Ger Offen DE 2,944,240
12. Yang R, Hu TD, Liu T, Xiang HW, Zhong B, Xu Y, Wu D (1998) Acta Phys-Chim Sin 14:590
13. Wang ZL, Liu QS, Yu JF, Wu TH, Wang GJ (2003) Appl Catal A Gen 239:87
14. Guerreiro ED, Gorriz OF, Rivarola JB, Arrúa LA (1997) Appl Catal A Gen 165:259
15. Bond GC, Namijo SN, Wakeman JS (1991) J Mol Catal 64:305
16. Zhang R, Sun YH, Peng SY (1999) React Kinet Catal Lett 67:95
17. Kozai S, Kabashima H, Hattori H (2000) Fuel 79:305
18. Damyanova S, Grange P, Delmon B (1997) J Catal 168:421
19. Huang ZT (2004) (ed) (China) Industry catalyst handbook. Chemical Industry Press, Beijing